

# SMALL&HIGH-SENSITIVE THREE AXIS SOI CAPACITIVE ACCELEROMETER

Non-member	Yasumasa Yamaguchi	(YAZAKI Corporation)
Non-member	Fumiharu Katsumata	(YAZAKI Corporation)
Non-member	Fumihiko Nishida	(YAZAKI Corporation)
Non-member	Masaaki Nishimura	(YAZAKI Corporation)
Member	Yoshinori Matsumoto	(Keio University)
Member	Makoto Ishida	(Toyohashi University of Technology)

The three axis SOI capacitive accelerometer has been developed using silicon bulk micro-machining. The accelerometer has a glass-silicon structure measuring 2.8mm by 2.8mm by 1.0mm. The accelerometer has a 500  $\mu$ m thick silicon mass formed by dicing using a SOI substrate. The accelerometer structure was released by R.I.E. process so that the sensor did not break or stick to the substrate. This process promises high throughput and high yield. The accelerometer was assembled with a switched-capacitor circuit and the characteristics were evaluated. The typical characteristics are as follows; Acceleration range is  $\pm 1.2G$ , sensitivity is 0.6V/G, cross-axis sensitivity is less than 7%.

Keywords: *capacitive, accelerometer, three axis, dicing saw, SOI*

## 1 INTRODUCTION

There is a great demand for low-cost and high-performance multi-axis accelerometers in automotive applications; ie. in airbags, anti-lock break systems, chassis controls. There has been a great deal of research involving micromachined accelerometers[1]-[3]. Most of them use wet etching processes for their mass formation. However, in general, wet processes result in low throughput and high cost.

In response to these problems, simple methods were pursued by many researchers, and a fabrication process using a dicing method was achieved [4]. In this work, a dicing saw was used for the mass formation because it required a high aspect ratio mass. However, it has not yet accomplished the sufficient productivity of the mass formation process. This paper describes the new process which was improved from above mentioned method and has more productivity. The characteristics of the new accelerometer evaluated with the switched-capacitor circuit are also described.

## 2 STRUCTURE

The schematic view of the three axis accelerometer is shown in Fig.1. The accelerometer has a glass-silicon structure

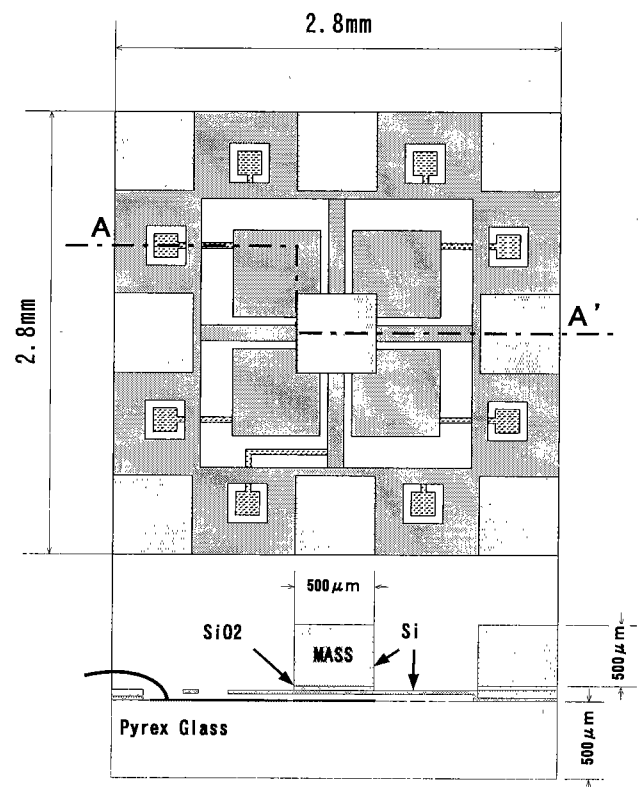


Fig1. Structure of accelerometer.

which has a mass of  $500 \mu\text{m}$  thickness formed with a dicing saw using a bulk silicon substrate. The mass is supported by four thin straight beams. The width and thickness of the beams were designed to be  $50 \mu\text{m}$  and  $10 \mu\text{m}$ , respectively. The gap between the mass and electrodes was  $2 \mu\text{m}$ . The Z-axis capacitance sensing electrodes are formed between the mass and metal electrode on the glass substrate. The X,Y-axis capacitance sensing electrodes are formed between a clover-leaf structure which is attached to the mass and metal electrodes on the glass substrate. The common electrode consists of the clover-leaf and the bottom surface of the mass. Facing against it there are 5 individual electrodes which are made separate by photolithography. The new accelerometer structure differs from the previous one [4] in two ways. First, the width of the dicing-line is  $500 \mu\text{m}$  which can be cut in one pass. Cutting in one pass doesn't generate the step of diced surface. It improves the sensor property and is more suitable for product than cutting in two pass. Second, pillars are remaining around the mass. These are advantage with packaging. The chip of the accelerometer was sealed to a ceramic package after die-bonding and wire-bonding. The lid of the ceramic package works as a stopper so that the mass didn't break by the over-range shocks.

### 3.SENSOR FABRICATION

#### 3.1 Mass formation with dicing saw

The dicing saw has been used to facilitate the formation of the mass of accelerometer because the dicing process makes it possible to fabricate the sensor at low cost and in a short time. So, we confirmed the possibility of high throughput by fabricating the accelerometer using a 4-inch wafer. Fig.2 shows the mass structure which is formed with the dicing saw.

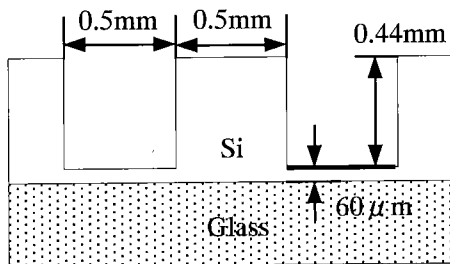


Fig.2 Diagram of mass formation with dicing saw.

When the remaining of silicon layer is less than  $60 \mu\text{m}$ , there are some micro-cracks generated. In order to improve the yield rate, the remaining of silicon layer is  $60 \mu\text{m}$ . Fig.3 shows the micro-cracks were generated on  $20 \mu\text{m}$  silicon remaining layer. If there are some micro-cracks on the layer, the sensor structure is in danger of destruction after dry process which follow the dicing process. Mass formation with the dicing saw was tested using  $512 \mu\text{m}$  thick silicon wafer at a rotor

speed of 30000r.p.m and stage speed of 1mm/sec with a blade of B1A801SD2000N100 M42(DISCO Co.). Fig.4 shows the photograph of silicon mass formed with the dicing saw with a blade of  $500 \mu\text{m}$  width. Fig.4 shows that the micro-cracks were not generated on the remaining of silicon layer and the dicing process has enabled the fabrication of a precise accelerometer mass.

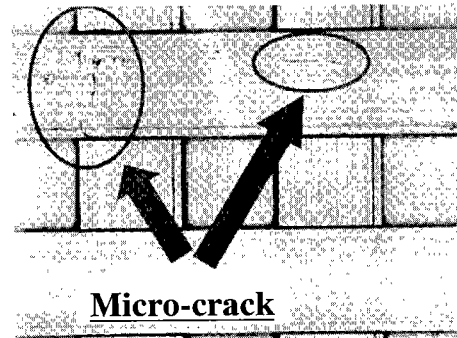


Fig.3 Photograph of micro-cracks by dicing.

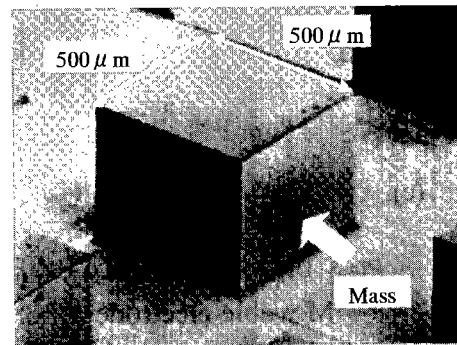


Fig.4 Photograph of silicon mass formed dicing saw with a blade of  $500 \mu\text{m}$  width.

#### 3.2 Mass release with dry process

In general, in the case of using a wet release process, beams stick to the substrate because of the surface tension. A dry process solved these problems and allowed high throughput. Fig.5 shows the mass release using the dry process. The process was designed as follows.

- (a) The remaining silicon layer was etched using the R.I.E. system with a gas mixture of  $\text{SF}_6$  and  $\text{O}_2$ . The selectivity against silicon dioxide was approximately 20. Therefore silicon mass was etched about  $3 \mu\text{m}$ . But this time we thought a certain level of silicon etching is inevitable. Fig.6 shows the silicon dioxide after etching the silicon remaining in the dicing process. Fig.6 shows that the beam and the movable electrode are supported by silicon dioxide. In this case the sensor structure did not break during the release process. Even if there was some roughness remained on the diced surface, it never affected the release process which is designed to stop on the silicon dioxide surface precisely.

(b) Next, silicon dioxide in the middle layer was etched with the R.I.E. system with a gas mixture of CHF<sub>3</sub> and O<sub>2</sub>. The selectivity against silicon was approximately 2.

(c) The accelerometer structure was released by a dry process so that the sensor did not break or stick to the substrate during the fabrication process. Fig.7 shows the photograph of accelerometer fabricated.

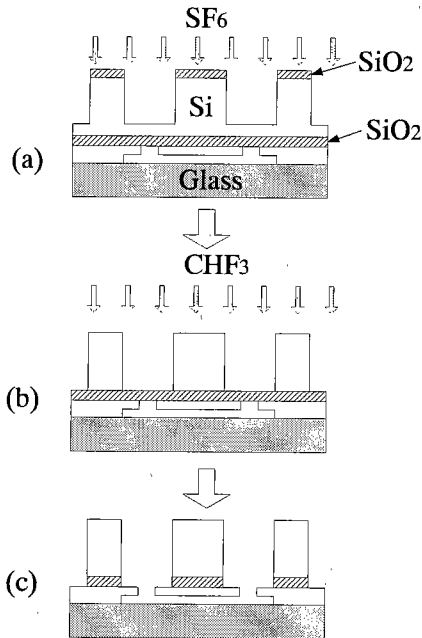


Fig.5 Dry release process.

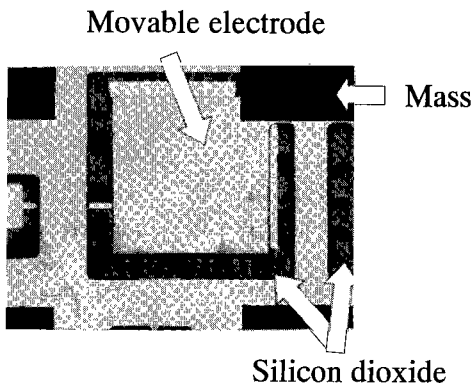


Fig.6 Photograph of silicon dioxide layer after etching the remaining silicon .

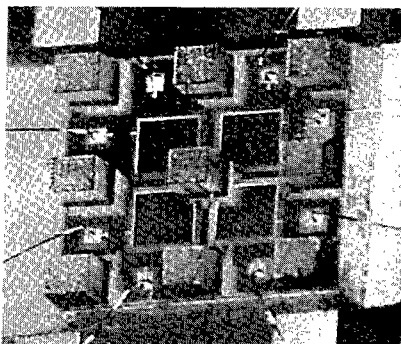


Fig.7 Photograph of a accelerometer fabricated.

#### 4 CAPACITANCE DETECTION CIRCUIT

The capacitive accelerometer, corresponding to the change of acceleration, converts the deformation of the gap formed between electrodes into a capacitance change. This capacitance change is too small in a few femto-farad of resolution. Therefore, a switched-capacitor circuit, which could eliminate stray capacitance and noise, was used. This diagram is shown in Fig.8.

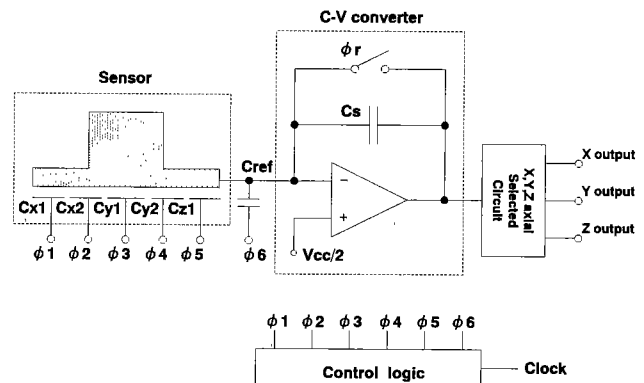


Fig.8 switched-capacitor type c-v converter for three-axis capacitive accelerometer.

It consists of three blocks; the switched-capacitor type C-V converter comprising the operational amplifier and analog switches, the control logic circuit and X, Y, Z axis selected circuit. C<sub>x1</sub> and C<sub>x2</sub> are charged by the phi 1 clock (Fig.9-a). Then, if the sensor capacitor is changed by acceleration, the output voltage V<sub>o</sub> is expressed by the equation (1) while C<sub>x1</sub> and C<sub>x2</sub> are unbalanced.

$$V_o = \frac{C_{x1} - C_{x2}}{C_s} \cdot V_{cc} + \frac{V_{cc}}{2} \quad (1)$$

Where C<sub>s</sub> is an integration capacitor. C<sub>x1</sub> and C<sub>x2</sub> are discharged during the phi 2, phi r clock (Fig.9-b). The output signal of the X axis is derived from this cycle. In the phi 3, phi 4 and phi r phase, the output signal of the Y axis is derived. Also, in the phi 5, phi 6 and phi r phase, the output signal of the Z axis is derived.

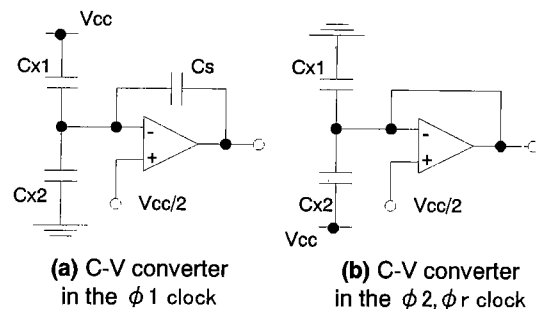


Fig.9 Circuit diagram of C-V converter.

Their signals are controlled using a time-sharing method. This time-sharing diagram is shown in Fig.10. And, several clocks ( $\phi 1 \sim \phi r$ ) are controlled by a control logic circuit. The X, Y, Z axis selection circuit is derived from the signals of several axis. Since this circuit use a switched-capacitor method, it is possible to fabricate an integrated circuit. The sensor electrodes are driven between  $V_{cc}$  and GND potential, and other electrode is fixed to  $V_{cc}/2$ . The electrostatic force caused by the detection circuit can be neglected if the  $\phi 1$  and  $\phi 2$  have same periods since the sensor structure acts as a mechanical low pass filter.

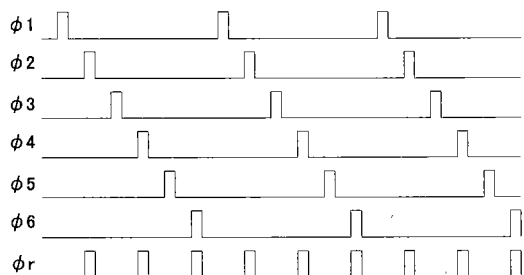


Fig.10 Timing diagram of the nonoverlapping six-phase clocks and reset-phase clock.

### 5 CHARACTERISTICS

The static characteristics of the sensor were measured using a rotary table. The relationship between the X output voltage without amplification in the circuit and the applied acceleration is shown in Fig.11. The output voltage has a linear dependence on the acceleration and the sensitivity was 28mV/G. Y and Z sensitivities were 27mV/G and 26mV/G, respectively. The specification sensitivities were 27mV/G (X,Y-axis) and 10mV/G (Z-axis). In consequence, X and Y sensitivities were almost as same as the specifications and Z sensitivity was more than two times the specifications. We supposed that Z sensitivity was better than the specifications, because the thickness of beam was thinner than the specifications.

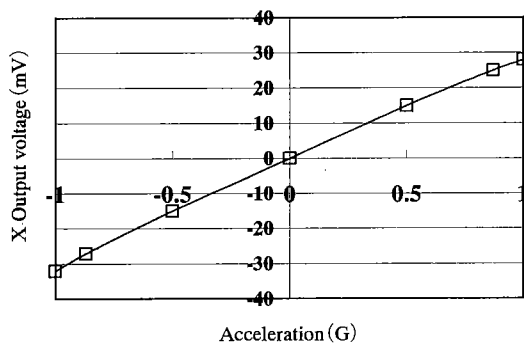


Fig.11 Output voltage versus acceleration.

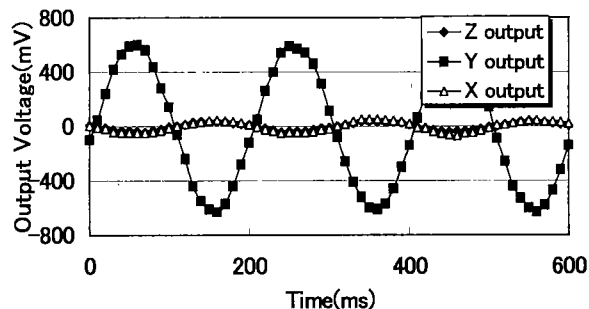


Fig.12 characteristics of accelerometer

The output voltages are amplified by a gain of 25, and filtered. Next, the dynamic characteristics of the sensor were measured using a low frequency measurement system. Fig.12 shows the performance for Y-axis acceleration of 1.2G at a frequency of 5Hz. The operating voltage is 5V. The sensitivity for the Y axis is 630mV/G and the cross axis sensitivity is less than 7%. The specification cross axis sensitivity was less than 1.8%.

### 6 CONCLUSION

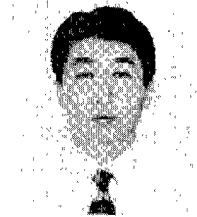
The three-axis SOI capacitive accelerometer was developed using silicon bulk micro-machining. To make the fabrication process of the accelerometer more productive, we improved the dicing process and the R.I.E. process. The dicing process did not generate any micro-cracks. The R.I.E. process did not brake the sensor structure. These processes promise high throughput and high yield. Characteristics of the accelerometer were evaluated with the switched-capacitor circuit. The typical characteristics are as follows; Acceleration range is  $\pm 1.2G$ , sensitivity is 0.6V/G, cross-axis sensitivity is less than 7%.

(Manuscript received June 16, 2000, revised Feb. 28, 2001)

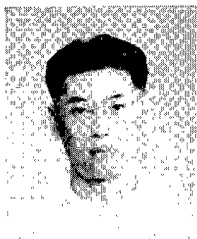
### REFERENCES

- [1] K.Okada, "development of tri-axial accelerometers using piezoresistance, electrostatic capacitance and piezoelectric elements", Tech.Dig.of the 13th Sensors Symposium, 1995, pp.169-172
- [2] T.Mineta, S.Kobayashi, Y.Watanabe, S.Kanauchi, I.Nakagawa, E.Suganuma, M.Esashi, "Three-axis capacitive accelerometer with uniform axial sensitivity", Proc.1995 Int. Conf. Solid State Sensors and Actuators (Tranducers'95), 1995, pp.554-557
- [3] O.Torayashiki, A.Takahashi, R.Tokue, "Capacitive type 3-axis accelerometer", Tech.Dig.of the 14th Sensor Symposium, 1996, pp.19-22.
- [4] K.Yoshida, Y.Matsumoto, M.Ishida, K.Okada, "High-sensitive three axis SOI capacitive accelerometer using dicing method", Tech. Dig. of the 16th Sensors Symposium, 1998, pp.25-28

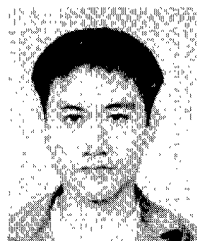
**Yasumasa Yamaguchi** (Non-Member) received a M.E. degree in electrical engineering from Toyota Institute of technology, Aichi, Japan, in 1995. Since 1989 he has been with YAZAKI Corporation. He is currently engaging in the development of sensors for automobile.



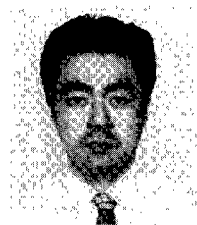
**Fumiharu Katsumata** (Non-Member) received a B.E. degree in electrical engineering from Yamanashi University, Yamanashi, Japan, in 1992. Since 1992 he has been with YAZAKI Corporation. He is currently engaging in the development of sensors for automobile.



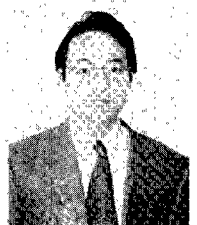
**Fumihiko Nishida** (Non-Member) received a M.E. degree in industrial engineering from Chuoh University, Tokyo, Japan, in 1996. Since 1997 he has been with YAZAKI Corporation. He is currently engaging in the development of sensors for automobile.



**Masaaki Nishimura** (Non-Member) received a M.E. degree in electrical and electronic engineering from Toyohashi University of Technology, Toyohashi, Japan, in 1997. Since 1997 he has been with YAZAKI Corporation. He is currently engaging in the development of sensors for automobile.



**Yoshinori Matsumoto** (Member) received his B.E. and Ph.D. degree in electronic engineering from Tohoku University, Sendai, Japan in 1988 and 1993, respectively. From 1993 to 1999, he was a research associate at the department of Electric and Electronic Engineering of Toyohashi University of Technology. Since 1999, he has been an assistant professor of the Department of Applied Physics and Physico-Informatics, Keio University. His research interests include integrated capacitive sensors, integrated circuits and optical devices.



**Makoto Ishida** (Member) was born in Hyogo, Japan, in 1950. He received the Ph.D. degree in electronics engineering from Kyoto University, Kyoto, Japan, in 1979. Since 1979 he has been at Toyohashi University of Technology, and he is a professor of electrical and electronic engineering. He is working on Si



related materials and devices, such as heteroepitaxial growth and processes of SOI material including epitaxial  $Al_2O_3$  insulator and Si films, and their device applications for advanced semiconductor devices including sensors and IC in electron device research center in Toyohashi University of Technology.